Crystallographic and Quantum Mechanical Results on Ψ[NHCO] Aliphatic Diamides. The Number of Methylenes Strongly Influences Their Structural and Conformational Properties

Eloísa Navarro, Carlos Alemán,* and Jordi Puiggalí*

Departament d'Enginyeria Química, ETS d'Enginyers Industrials, Universitat Politècnica de Catalunya, Diagonal 647, Barcelona 08028, Spain

Received February 21, 1997; Revised Manuscript Received July 17, 1997[⊗]

ABSTRACT: The crystal structures of four diamides represented by the general formula $CH_3-CONH(CH_2)_nNHCO-CH_3$ ($n = 2-5$) were solved by X-ray diffraction in order to establish the conformational preferences of the polymethylene segments. The results are complementary of our previous works on diamides and diketones where the conformation of the dicarbonylic units were established. The results appear useful to study the conformation of related compounds, as polyamides, where the experimental data are scarce. A folding trend of the polymethylene segment, when the number of methylenes is less than 4, can be deduced. The same conclusions were inferred from *ab initio* quantum mechanical calculations at the MP2/6-31G(d)//HF/6-31(d) level.

Introduction[1]

A systematic effort has been recently carried out to investigate the structure of aliphatic polyamides. More specifically, to relate them with the well-known structures found in polypeptides. Thus, polyamides with helical conformations similar to the intramolecular[2,3] (α-helix) or to the intermolecular[3−5] (PG II structure) hydrogen-bonded structures, characteristic of polypeptides, have been attained. Due to the scarce amount of data available for synthetic polymers, these structures have been supported with crystallographic[6−8] data and *ab initio* quantum mechanical calculations[9,10] on model compounds. Unusual folded conformations for diacid derivatives[8−14] as well as slight deviations from the *all-trans* conformations for ω-amino acid derivatives[7] have been found. These results deserve further considerations on macromolecular chemistry, which can be summarized as follows.

1. Dicarbonylic derivatives are characterized by a *gauche* conformation for the bond defined by the first and second carbon atoms next to the carbonyl groups.[8−10,15] The same trend has frequently been observed in the side chains of glutamine and asparagine residues of both small peptides[14,16,17] and proteins.[14,16,18] This *gauche* conformation is in contradiction with force-field calculations based on empirical potentials, which indicate a *trans* conformation and suggest an erroneous parametrization of such residues. Repercussions on the structural determination of proteins with a low resolution are obvious.

2. The rigid *all-trans* conformation usually considered for polymethylene segments would be doubtful as it was also conclusively demonstrated from the librational motion found in nylon 6,6 by molecular dynamics simulations and experimental NMR spectroscopy.[19] Furthermore, the refinement of some polyamides like nylons *n,3* was considerably improved when the polymethylene segment was allowed to deviate from the *all-trans* conformation.[13]

3. The conventional sheet structures of nylons are characterized by a single hydrogen bond direction.[20] However, different assumptions with two or three hydrogen bond directions have actually been done for (a) quenched samples,[21] (b) polyamides over their Brill transition temperature,[22] and (c) some specific nylons derived from dicarboxylic acids with a low number of methylene groups.[23,24] The folded conformations found in the analysis of model compounds explain this peculiar behavior, since repulsive interactions between the carbonyl oxygen atoms favor the conformations where amide groups are twisted, allowing more than one hydrogen bond direction.

In this work, we complete our previous works carried out for the dicarbonylic units. The conformational preferences of a series of *N,N′*-oligomethylenedialkylamides [$R-CONH(CH_2)_nNHCO-R$, $R = CH_3$, $n = 2-5$] have been explored in the solid state using X-ray crystallography and *in vacuo* using *ab initio* quantum mechanical calculations. Up to date, only aromatic derivatives have been studied in the solid state as model compounds of terephthalamides.[17] Since packing interactions between aromatic rings may influence the molecular conformation in solid state,[11] the study of methyl derivatives becomes fundamental to the understanding of the intrinsic conformational preference of the polymethylene segments of diamine compounds. The results are an extension of our previous findings about the folding of methylene units and appear useful to simulate the respective structure of nylons containing both diamine and diacid units.

Experimental Section

Characterization. Infrared (IR) spectra were obtained from KBr pellets using an IRTF Perkin-Elmer 1600 spectrophotometer in the 4000−500 cm^{-1} range. Proton and carbon magnetic resonance (^1H and ^{13}C) spectra were obtained in deuterated solvents as chloroform, dimethyl sulfoxide, or trifluoroacetic acid using a Bruker AMX-3000 spectrometer. Chemical shifts are reported in parts per million (δ) downfield from internal standard tetramethylsilane (TMS). Chromatographic purity was determined with an HPLC Shimadzu SCL-6B analyzer, using an RP-18 Spherisorb ODS-2 column (25 ×

* To whom correspondence should be addressed.

[⊗] Abstract published in *Advance ACS Abstracts,* December 15, 1997.

S0024-9297(97)00243-X CCC: $15.00 © 1998 American Chemical Society
Published on Web 01/08/1998

Table 1. Crystalization Conditions

compound	concentration (mg/mL)	$CHCl_3$/ether proportions		ether
		solvent	precipitant	
aETa	1.0	5.8/4.2	5.5/4.5	dibutyl
aPRa	1.0	1/1	2/3	dibutyl
aBUa	1.0	3/2	1/1	diethyl
aPEa	1.0	3/2	5.5/4.5	dibutyl

0.4 cm; particle size, 5 μm). The column was eluted with 50% MeOH in water, and the flow rate was kept at 1 mL/min (λ = 210 nm).

Synthesis. Compounds were obtained through the reaction of the appropriate diamine (50 mmol) with acetic anhydride (200 mmol) in a tetrahydrofuran-water mixture (9:1) solution.[25] Triethylamine (200 mmol) was added in all cases as a proton acceptor. The compounds were recrystallized from $CHCl_3$/EtOEt, giving white powders with 33, 62, 35, and 42% yield for the **et**hylene, **pr**opylene, **bu**tylene, and **pe**ntylene derivatives, respectively.

***N*-[2-(Acetylamino)ethylene]acetamide (aETa).** Mp = 175−178 °C (uncorrected). IR (KBr, ν, cm^{-1}): 3294, 3090, 2984, 2934, 2862, 1654,1560, 1446, 1366, 1288, 1249, 1105, 1039, 1001, 931, 746, 629, 606. ^{1}H NMR (DMSO-d_6, 300.1 MHz, δ, ppm): 1.79 (s, 6H, $-CH_3$), 3.04 (d, 4H, $-CH_2-$), 7.89 (m,2H, −NH−). ^{13}C NMR ($CDCl_3$, 75.5 MHz, δ, ppm): 22.54 ($-CH_3$), 38.28 ($-CH_2-$), 169.23 (−CO−). HPLC chromatographic purity: 98%, elution time: 2.70 min.

***N*-[3-(Acetylamino)propylene]acetamide (aPRa).** Mp = 101−104 °C (uncorrected). IR (KBr, ν, cm^{-1}): 3280, 3094, 2977, 2948, 2886, 1635, 1552, 1484, 1450, 1369, 1296, 1263, 1127, 756, 718, 632, 610, 600. ^{1}H NMR ($CDCl_3$, 300.1 MHz, δ, ppm): 1.57 (quint, 2H, $-CH_2CH_2CH_2-$), 1.93 (s, 6H, $-CH_3$), 3.20 (q, 4H, $-NHCH_2-$), 6.64 (m, 2H, −NH−). ^{13}C NMR ($CDCl_3$, 75.5 MHz, δ, ppm): 22.93 ($-CH_3$), 29.26 ($-NHCH_2CH_2-$), 35.93 ($-NHCH_2-$), 170.78 (−CO−). HPLC chromatographic purity: 98.8%. Elution time: 3.10 min.

***N*-[4-(Acetylamino)butylene]acetamide (aBUa).** Mp = 141−142 °C (uncorrected). IR (KBr, ν, cm^{-1}): 3301, 3074, 2950, 2879, 1634, 1542, 1486, 1364, 1295, 1102, 1044, 957, 715, 600, 513. ^{1}H NMR (TFA-*d*, 300.1 MHz, δ, ppm): 1.80 (m, 4H, $-NHCH_2CH_2-$), 2.50 (s, 6H, $-CH_3$), 3.60 (m, 4H, $-NHCH_2-$). ^{13}C NMR (TFA-*d*, 75.5 MHz, δ, ppm): 20.76 ($-CH_3$), 26.60 ($-NHCH_2CH_2-$), 43.83 ($-NHCH_2-$), 179.13 (−CO−). HPLC chromatographic purity: 97.8%. Elution time: 3.57 min.

***N*-[5-(Acetylamino)pentylene]acetamide (aPEa).** Mp = 129−131 °C (uncorrected). IR (KBr, ν, cm^{-1}): 3294, 3090, 2984, 2934, 2862, 1654, 1560, 1446, 1366, 1288, 1249, 1105, 1039, 1001, 931, 746, 629, 606. ^{1}H NMR ($CDCl_3$, 300.1 MHz, δ, ppm): 1.28 (quint, 2H, $-NH(CH_2)_2CH_2-$), 1.46 (quint, 4H, $-NHCH_2CH_2-$), 1.91 (s, 6H, $-CH_3$), 3.16 (q, 4H, $-NHCH_2-$), 5.86 (s, 2H, −NH−). ^{13}C NMR ($CDCl_3$, 75.5 MHz, δ, ppm): 23.22 ($-CH_3$), 23.65 ($-NH(CH_2)_2CH_2-$), 28.89 ($-NHCH_2CH_2-$), 39.09 ($-NHCH_2-$), 170.41 (−CO−). HPLC chromatographic purity: 97%. Elution time: 4.02 min.

X-ray Diffraction. Crystals suitable for X-ray diffraction were obtained by vapor diffusion of $CHCl_3$/ether solutions against mixtures enriched in ether which were used as precipitants. Table 1 summarizes the crystallization conditions. X-ray data were collected at room temperature using an Enraf-Nonius CAD4 diffractometer with Cu Kα graphite-monochromatized radiation (λ = 1.541 78 Å). Cell parameters were refined by least squares on the basis of 25, 20, 20, and 25 independent reflections for **aETa**, **aPRa, aBUa**, and **aPEa**, respectively. Three reflections were monitored every hour during data collection and showed that fluctuation of intensity was less than 2%, except for **aPRa** which showed a 7% decay. **aETa**, **aBUa**, and **aPEa** intensity data were corrected for Lorentz and polarization effects but not for absorption, whereas **aPRa** intensity data was also corrected for absorption. The structures were solved by direct methods using the SHELXS-86[26] computer programs package and assuming a $P\bar{1}$, $P12_1/n1$, $P\bar{1}$, and *Pbcb* symmetry for **aETa**, **aPRa, aBUa**, and **aPEa**, respectively. The E-maps were calculated and revealed all the non-hydrogen atoms. The molecular structures were then refined by a full-matrix least-squares procedure (SHELXL-93[27]) with weights redetermined after each program run. In all cases cycles of refinement and difference Fourier syntheses showed only some of the hydrogen atoms. Those bonded to the N atoms were placed in the positions found in the difference Fourier maps. The remaining hydrogen atoms were placed in stereochemically ideal positions and refined with geometrical constraints ("ride model"). Anisotropic full-matrix refinement for non-hydrogen atoms and isotropic for hydrogens

Table 2. Crystallographic Data

compound	**aETa**	**aPRa**	**aBUa**	**aPEa**
molecular formula	$C_6H_{12}N_2O_2$	$C_7H_{14}N_2O_2$	$C_8H_{16}N_2O_2$	$C_9H_{18}N_2O_2$
crystal size (mm^3)	0.2 × 0.2 × 0.1	0.3 × 0.2 × 0.1	0.3 × 0.12 × 0.04	1.8 × 0.2 × 0.1
crystal system	triclinic	monoclinic	triclinic	orthorhombic
space group	$P\bar{1}$	$P12_1/n1$	$P\bar{1}$	*Pbcb*
cell				
a (Å)	4.909 (1)	10.800 (2)	4.892 (1)	5.39 (2)
b (Å)	6.847 (1)	4.806 (1)	5.264 (1)	8.86 (6)
c (Å)	7.083 (1)	17.078 (4)	9.339 (2)	22.335 (7)
α (deg)	116.78 (1)	90.00 (1)	87.86 (1)	90.00 (2)
β (deg)	104.67 (1)	99.40 (2)	89.53 (1)	90.00 (5)
γ (deg)	90.65 (1)	90.00 (2)	88.38 (1)	90.00 (2)
volume ($Å^3$)	203 (2)	874 (2)	240 (1)	1066 (3)
Z (no. of asymetric units)	2	4	2	8
asymmetric unit (molecule)	1/2	1	1/2	1/2
calculated density (g/cm^3)	1.177	1.202	1.191	1.160
scanning mode	$\omega/2\theta$ scan	$\omega/2\theta$ scan	ω scan	ω scan
collected reflections	831 (2θ < 136°)	3580 (2θ < 136°)	962 (2θ < 136°)	3912 (2θ < 136°)
unique reflections	736	1501	849	982
R(int)	0.0067	0.025	0.005	0.062
$R(\sigma)$	0.0149	0.021	0.014	0.040
observed reflections	588 ($I > 2\sigma(I)$)	1313 ($I > 2\sigma(I)$)	638 ($I > 2.5\sigma(I)$)	813 ($I > 2.5\sigma(I)$)
no, of refined parameters	62	157	66	96
goodnes-of-fit on F^2	0.976	0.783	1.020	0.933
R factor	0.078	0.071	0.078	0.071
wR^2	0.221[a]	0.191[b]	0.223[c]	0.197[d]
min/max heights ($e/Å^3$) in the difference Fourier map	0.31/−0.30	0.31/−0.26	0.26/−0.25	0.30/−0.21

[a] $1/w = \sigma^2(F_o^2) + (0.1827P)^2 + 0.09P$ where $P = [\max(F_o^2,0) + 2F_c^2/3]$. [b] $1/w = \sigma^2(F_o^2) + (0.210P)^2 + 0.37P$ where $P = [\max(F_o^2,0) + 2F_c^2/3]$. [c] $1/w = \sigma^2(F_o^2) + (0.155P)^2 + 0.16P$ where $P = [\max(F_o^2,0) + 2F_c^2/3]$. [d] $1/w = \sigma^2(F_o^2) + (0.167P)^2 + 0.47P$ where $P = [\max(F_o^2,0) + 2F_c^2/3]$.

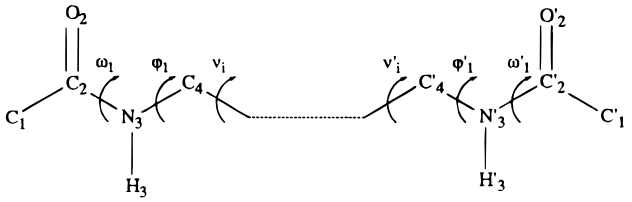

Figure 1. Atomic numbering and torsion angles for the model compounds studied in this paper.

converged to the standard agreement factors indicated for the four structures in Table 2. The atomic scattering factors were taken from the International Tables for X-ray Crystallography (1974) and a micro-Vax 2000 computer was used for all the calculations.

Quantum Mechanical Calculations. Minimum-energy conformations for **aETa** and **aPRa** were obtained by geometry optimizations at the Hartree−Fock level using the standard 6-31G(d)[28] basis set. Force constant analysis was carried out to verify the minimum nature of the optimized conformations as well as to obtain the ZPE and to make the thermal corrections. Basis set and electron correlation effects on **aETa** were estimated by single-point calculations at the HF/6-31+G-(d) and MP2/6-31+G(d)[29] levels, respectively. Thus, a combination of MP2/6-31+G(d)//HF/6-31G(d) (level of energy calculation//level of geometry optimization) with the HF/6−31G(d) frequencies gives our best estimations of the conformational energies. All the calculations were performed with the Gaussian-94 program[30] on a SP2 computer of the Centre de Supercomputación de Catalunya (CESCA).

Results and Discussion

A schematic representation of the model molecules **aETa, aPRa**, **aBUa**, and **aPEa** is shown in Figure 1 together with the definition of internal rotation angles, while stereoscopic views of the four conformations found by X-ray crystallography for the molecules are shown in Figure 2. The list of final atomic coordinates and their estimated standard deviations are given as Supporting Information. Final molecular parameters as selected internal rotation angles and hydrogen bond geometry are reported in Tables 3 and 4. It should be noted that the use of primed symbols does not imply the presence of a symmetry element along the chain. Experimental values for bond distances and bond angles are consistent with known literature data for amide groups and paraffin chains. Thus, in all cases the amide group is almost planar, being the root-mean-square distance of the atoms from the average plane less than 0.0042, 0,022−0.029, 0.0003, and 0.022 Å for **aETa, aPRa**, **aBUa**, and **aPEa**, respectively.

***N*-[(2-(Acetylamino)ethylene]acetamide (aETa).** A representation of the crystalline structure of **aETa** is given in Figure 3. The molecular symmetry is characterized by an inversion center in the middle of the ethylene segment. A system of linear and intermolecular hydrogen bonds characterizes also the crystalline structure. Thus, each molecule is hydrogen bonded, along the *a* direction, with two neighboring molecules. In this sense the structure differs from the data reported for the related compound *N*,*N*′-ethylenedibenzamide,[31] where the hydrogen-bonding interactions are established between one molecule and its four neighboring molecules. The molecular conformation is characterized by a φ torsion angle value around 90° which strongly deviates from the expected *trans* conformation. Such behavior seems to be an intrinsic characteristic of the molecule since hydrogen bonds are expected to be equal or better with the extended conformation characteristic

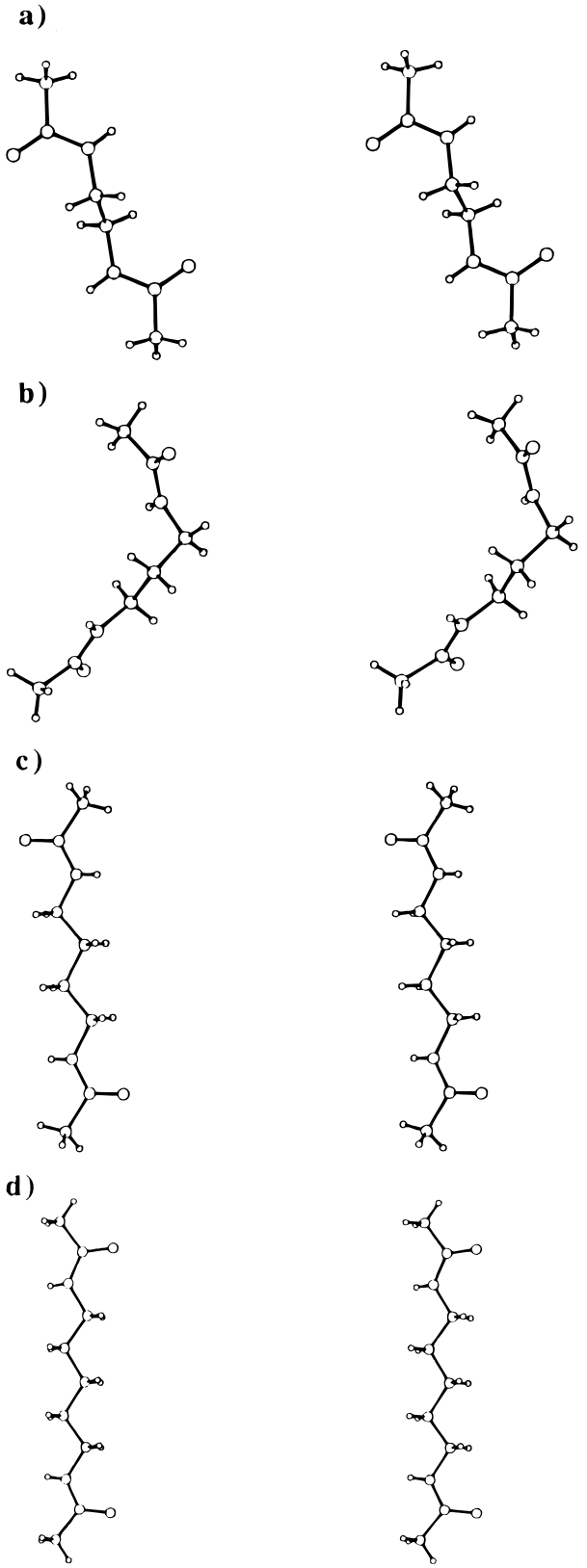

Figure 2. Stereopairs showing the conformation in the solid state of the model molecules: **aETa** (a), **aPRa** (b), **aBUa** (c), and **aPEa** (d). Note the folded conformation of the propylenediamine moiety and the rotation between the N−H directions in the pentylenediamine moiety.

of the α form of nylons. The φ torsion angle is relatively close to the *skew* conformation characteristic of the γ form of nylons, which is however expected to be favored

Table 3. Selected Torsion Angles (deg)

angle	aETa	aPRa	aBUa	aPEa
ω_1	179.2 (2)	177.0 (2)	180.0 (2)	−178.3 (2)
φ_1	93.2 (4)	175.2 (2)	172.5 (2)	−166.5 (2)
ν_1	180.0 (2)	172.8 (2)	180.0 (2)	180.0 (2)
ν_2			180.0 (2)	178.9 (2)
ν_2'				178.9 (2)
ν_1'		−74.6 (2)	180.0 (2)	180.0 (2)
φ_1'	−93.2 (4)	−94.4 (2)	−172.5 (2)	−166.5 (2)
ω_1'	−179.2 (2)	174.4 (2)	180.0 (2)	−178.3 (2)

Table 4. Hydrogen Bond Geometry for the Model Compounds

	aETa	aPRa	aBUa	aPEa
$d(H_3\cdots O_2)$ (Å)	1.98		2.16	2.07
$d(N_3\cdots O_2)$ (Å)	2.82		2.91	2.91
$\angle(N_3H_3\cdots O_2)$ (deg)	168		171	166
$d(H_3\cdots O'_2)$ (Å)		2.13,[a] 2.13[b]		
$d(N_3\cdots O'_2)$ (Å)		2.88,[a] 2.91[b]		
$\angle(N_3H_3\cdots O'_2)$ (deg)		176,[a] 169[b]		

[a] Hydrogen bonds established between molecules related by a 2-fold screw axis. [b] Hydrogen bonds established between molecules related by an inversion center.

for long polymethylene segments due to the improvement of the van der Waals interactions.

Similar conformational angles have been found for the model compounds available in Cambridge Structural Data Base.[17] Thus, values for the φ angle around 88.8°, 85.7° and 82.6° have been reported for *N,N′*-ethylenedibenzamide,[31] *N,N′*-bis(2′-pyridinecarboxamide)-1,2-ethane,[32] and diethyl *N,N′*-ethylenediaminobis(4-oxobutenoate),[33] respectively.

The intrinsic conformational preferences of **aETa** have been investigated using *ab initio* quantum mechanical calculations. A complete exploration of the conformational space has been performed at the HF/6-31G(d) level. Since each of the three backbone torsion angles (φ_1, ν, and φ_1' in Figure 1) are expected to have three minima, 27 minima may be anticipated for the potential energy hypersurface $E = E(\varphi_1,\nu,\varphi_1')$. However, due to the chemical and molecular symmetry of the compound, the number of conformations required as starting points in geometry optimizations is reduced. In order to obtain a more accurate estimation of the relative energies, single-point calculations at the HF/6-31+G(d) and MP2/6-31+G(d) were performed on all minima found. Results are displayed in Table 5.

Note that for all minima found at least one of the torsion angles φ_1 and φ_1' adopts a folded conformation, i.e., *skew* or *gauche*. Indeed, only two of six minima characterized (minima **1** and **6**) retain an almost extended conformation in φ_i angle. This structure is the less favored conformation at the computative levels used, being 6.9 kcal/mol unstabilized with respect to the lowest energy minimum. A striking feature is the large influence of electron correlation on conformational energies. Thus, the relative energy order between the different conformers estimated at the HF level is changed with respect to that estimated at the MP2 level. An inspection to the different minima depicted in Figure 4 permits one to clarify these results. Minima **1** and **5** are stabilized by an intramolecular seven-membered hydrogen bond system (C_7 conformation). These two minima have an asymmetric behavior on the φ_1 and φ_1' dihedral angles, which must be attributed to the tendency to form the intramolecular hydrogen bond. The C_7 intramolecular hydrogen bond geometries for **1** and **5** are characterized by [$R_{H\cdots O}$ = 2.16 Å, <N−H···O = 142.8°] and [$R_{H\cdots O}$ = 2.84 Å, <N−H···O = 100.9°]. These hydrogen bond parameters correlate well with the relative energies of **1** and **5**. Thus, the former is the lowest energy conformation at the HF level, whereas the latter is unfavored by about 1.7 kcal/mol at the same computational level.

Inspection of minimum **2** in Figure 4 permits one to understand the dramatic influence of electron correlation on conformational energies. Note that this structure is stabilized by the antiparallel stacking of the amide groups. Thus, it is well-known that electron correlation effects are required in order to provide a reliable description of the stacking interactions.[34] Minimum **4** seems to be basically stabilized by the interactions between the dipole moments of the amide groups. Minimum **3** corresponds to the conformation determined for **aETa** by X-ray crystallography. This conformation is unfavored with respect to the global minimum by 0.7 and 3.0 kcal/mol at the HF and MP2 levels, respectively. Note that **3** has an optimum conformation to form infinite networks of hydrogen bonds, and therefore it should be stabilized in the solid state. Unfortunately, packing interactions cannot be introduced in our theoretical calculations, due to computational limitations. Finally, it should be noted that the *all-trans* conforma-

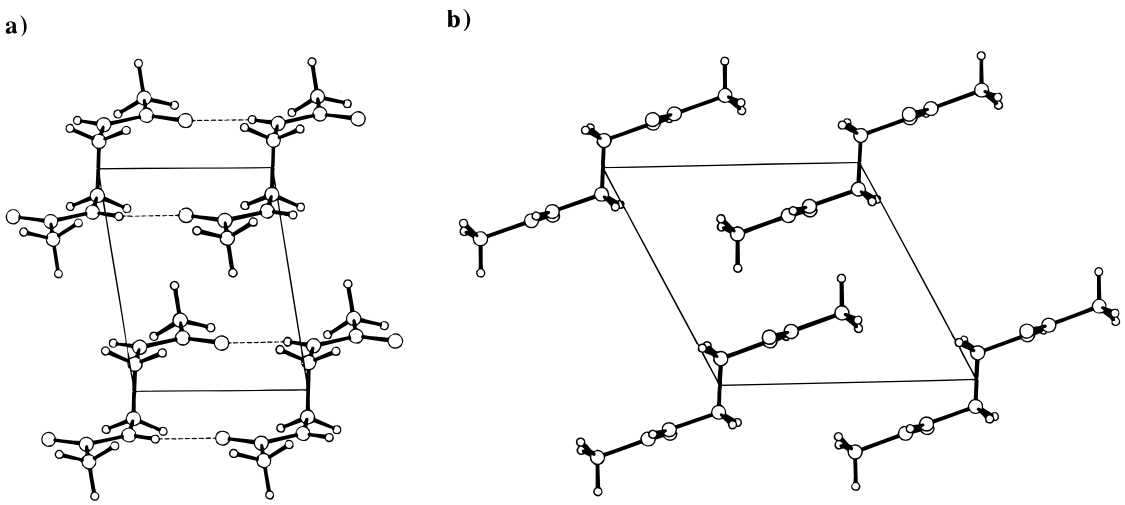

Figure 3. Projections of the crystalline structure of **aETa** onto the *ab* plane (a) and the *bc* plane (b). The unit cell is shown by thinner lines. Hydrogen bonds are established along the *a* direction and are indicated by dashed lines.

Table 5. *Ab Initio* Dihedral Angles (deg) and Relative Energies (kcal/mol) of aETa Minimun-Energy Conformations[a]

	ω_1	φ_1	ν_1	φ'_1	ω'_1	ΔE^b (HF/6-31G(d))	ΔE^b (HF/6-31+G(d))	ΔE^b (MP2/6-31+G(d))
1	−175.8	−177.1	−66.2	88.8	−179.0	0.0	0.0	1.2
2	17.3	−91.1	59.8	−91.1	170.2	0.0	0.8	0.0
3	−176.8	−80.4	180.0	80.3	177.0	1.0	0.7	3.0
4	175.1	77.5	59.5	77.6	174.9	1.3	1.1	2.6
5	−171.1	−93.8	68.5	77.3	−165.1	1.9	1.7	3.1
6	174.3	153.1	177.5	92.9	179.5	4.2	4.1	6.9

[a] Minimun energy conformers in the HF/6-31G(d) potential energy hypersurface. [b] Includes ZPE and thermal corrections computed at the HF/6-31G(d) level.

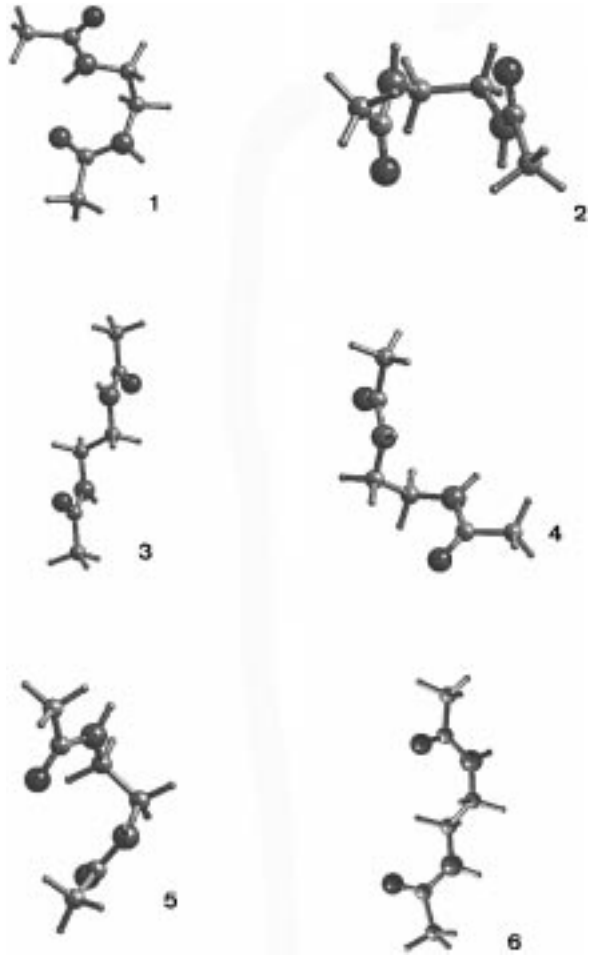

Figure 4. Minimum-energy conformations of *N*-[2-(acetylamino)ethylene]acetamide, numbering is according to Table 5.

tion has not been characterized as a minimum in the potential energy hypersurface of **aETa**. Thus, a geometry optimization of the *all-trans* conformation leads to minimum **3**, which is the conformation experimentally observed. However, its conformational energy was computed at the HF/6-31G(d) level by holding the φ_1, ν, and φ'_1 torsion angles fixed at 180.0°, while all the other geometrical parameters were relaxed. The final structure was less stable than **1** by 4.7 kcal/mol.

***N*-[(3-(Acetylamino)propylene]acetamide (aPRa).** In spite of the symmetry configuration of the **aPRa** molecule, the solid-state conformation becomes asymmetric as deduced from the different values of the φ_1 and φ'_1 or ν_1 and ν'_1 torsion angles. The propylenediamine moiety takes a $TT\bar{G}\bar{S}$ (or $TTGS$) folded conformation which induces a ca. 141.14° rotation between its two N−H directions. This peculiar conformation is similar to that found in the unique acyclic propylenediamine derivative which appears on literature. Thus, values of −140.3°, 176.1°, 64.1°, and 87.4° for φ_1, ν_1, ν'_1 and φ'_1 torsion angles have been reported for the *N*,*N*′-trimethylenedibenzamide[35] compound. These results suggest that the TG conformation is characteristic of the aliphatic segment. In the same way as the butylenediamide derivatives (next section) the aliphatic or aromatic nature of the substituent attached to the amide groups influences preferentially the φ_i torsion angles.

aPRa crystallizes in a $P12_1/n1$ space group with four molecules per unit cell (Figure 5). Two of them are related by a 2-fold screw axis, whereas the other two are generated by an inversion center and so their torsion angles have opposite signs. The packing is essentially different from that of other related diamides: each molecule is connected by hydrogen bonding to three others. Two identical hydrogen bonds are established with the neighboring chain related by the inversion center symmetry, and two additional hydrogen bonds are established with the two neighboring chains related by the screw axis. As can be seen in Table 4, the two kinds of hydrogen bonds are slightly different, being more linear than the hydrogen bonds established between molecules related by helical symmetry. It is worth noting that the packing of the *N*,*N*′-trimethyldibenzamide[35] related compound is quite different, with each molecule being in this case associated with two others through hydrogen bonding. A different packing where each molecule is hydrogen bonded to its four neighbors has also been described for *N*,*N*′-pentamethyldibenzamide,[35] *N*,*N*′-bis(β-chloroethyl)glutaramide,[36] and *N*,*N*′-bis(β-chloroethyl)pimelamide.[37]

The large size of **aPRa** precludes a complete exploration of its conformational space at the *ab initio* level. Therefore, only some selected geometries were used as starting points in geometry optimizations. The effect of electron correlation was investigated using a computational strategy previously applied to other related size compounds.[9,38] Thus, single-point calculations at the MP2/6-31G level were performed on the HF/6-31G(d) optimized geometries. Then, for each conformation the correlation contribution computed at the MP2/6-31G level was added to the HF/6-31G(d) energy. Results are summarized in Table 6.

The starting conformations in geometry optimizations were the structure found for *N*,*N*′-dipropylglutaramide,[9] the extended conformation, and the structure found in the present work for **aPRa**, which converge to minima **7**, **8**, and **9**, respectively. These minimum-energy conformations are schematically depicted in Figure 6. Note the large conformational flexibility of the methylene segment, which is folded in all the structures. The lowest energy conformation corresponds to $\bar{S}GG\bar{S}$ structure, which is very similar to the minimum **2** found for **aETa**. This structure is strongly favored by an antiparallel stacking of the amide group and therefore

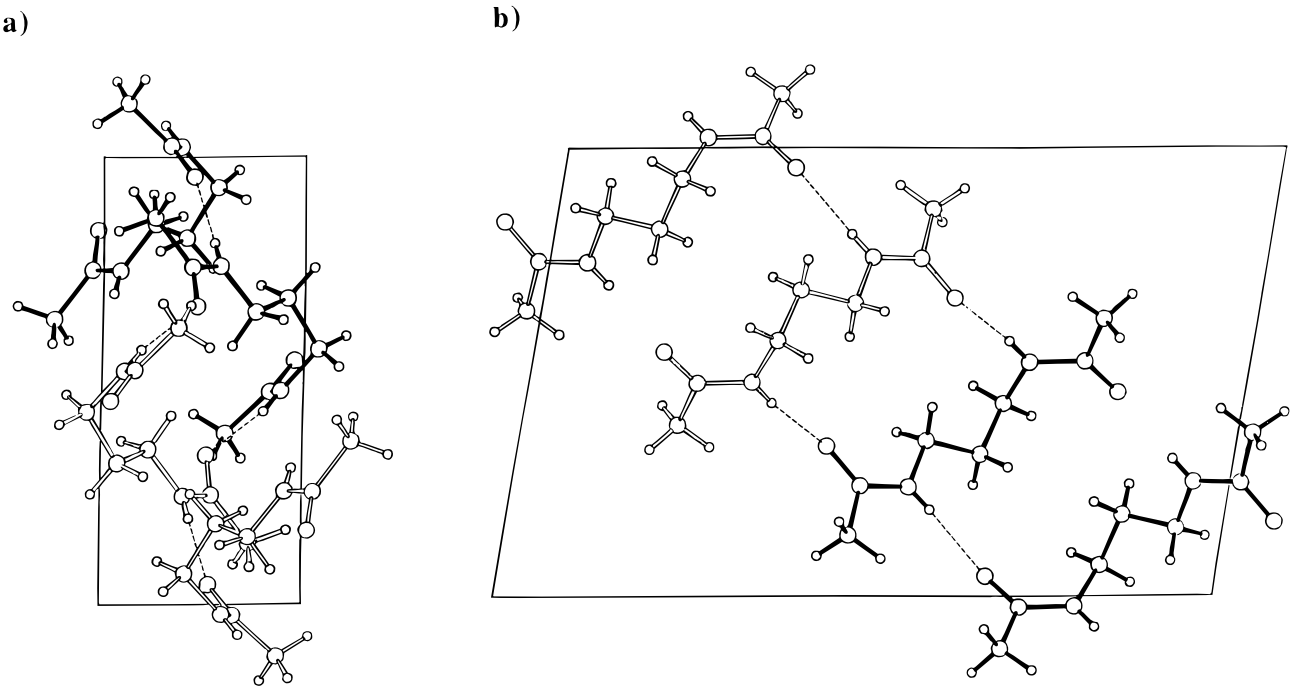

Figure 5. Projections of the crystalline structure of **aPRa** onto the *ab* plane (a) and the *ac* plane (b). Hydrogen bonds are established along the *a* direction and are indicated by dashed lines. Molecules with identical conformation had been indicated with the same kinds of bonds (white or black).

Table 6. *Ab Initio* Dihedral Angles (deg) and Relative Energies (kcal/mol) of aPRa Minimun Energy Conformations[a]

	ω_1	φ_1	ν_1	ν'_1	φ'_1	ω'_1	ΔE^b (HF/6-31G(d))	ΔE^b (HF/6-31G(d))+MP2
7	173.9	−121.7	51.4	51.3	−121.7	173.9	0.00	0.00
8	175.7	−82.9	179.6	179.6	−83.1	175.4	0.54	2.00
9	174.1	166.7	−179.7	−63.9	−81.0	−176.3	1.34	2.88

[a] Minimun energy conformers in the HF/6-31G(d) potential energy hypersurface. [b] Includes ZPE and thermal corrections computed at the HF/6-31G(d) level.

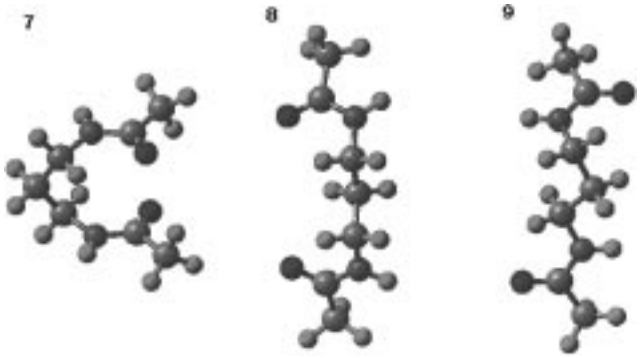

Figure 6. Minimum energy conformations of *N*-[3-(acetylamino)propylene]acetamide obtained from selected starting conformations. Numbering is according to Table 6.

strongly stabilized by electron correlation effects. Structure **8** results from geometry optimization of the *all-trans* conformation and corresponds to the $\bar{G}TT\bar{G}$. This structure was 2.0 kcal/mol less stable than **7** and is similar to the so-called γ form of nylons. Geometry optimization of the *TGGT* conformation leads to **7**, indicating that such a structure is not an energy minimum on the potential energy surface of **aPRa**. Finally, minimum **9** corresponds to the conformation found in the solid state. It is only 0.9 kcal/mol less favored than **8**. Although the *all-trans* conformation was not found as a minimum, its conformational energy was computed by keeping all the φ_i and ν_i values fixed, while all the other geometrical parameters were relaxed. The all-*trans* conformer was 1.7 kcal/mol less stable than **9** at the HF/6-31G(d) level. These results clearly indicate that in **aPRa** the methylene segment tends to fold to adopt a conformation able to form an infinite network of hydrogen bonds. Such a conformation in the solid state is stabilized by cooperative effects which overcome the intramolecular interactions found in **7**.

***N*-[4-(Acetylamino)butylene]acetamide (aBUa).** **aBUa** crystallizes in a $P\bar{1}$ space group, with the molecular symmetry being characterized by an inversion center in the middle of the polymethylene segment. Thus, the torsion angles of the half molecules are identical but with opposite signs. The main features of the **aBUa** structure are in good agreement with the α form of nylons. So, the resulting chain conformation is practically *all-trans* and a sheet structure with a single hydrogen bond direction can be envisaged. Hydrogen-bonded molecules are shifted along the molecular axis (Figure 7) in order to optimize the hydrogen bond geometry, whereas consecutive sheets are shifted along the hydrogen bond and in the chain axis directions in order to improve both the van der Waals and dipole−dipole interactions. It is worth noting the slight deviation from 180° observed for the φ_1 and φ'_1 torsion angles, giving support to the idea that similar deviations should be taken into account when the structure of related polymers, as nylons, is modeled. Similar deviations around the extended-chain value for the polymethylene segment have also been postulated for nylons above the Brill transition temperature. Previous data on buty-

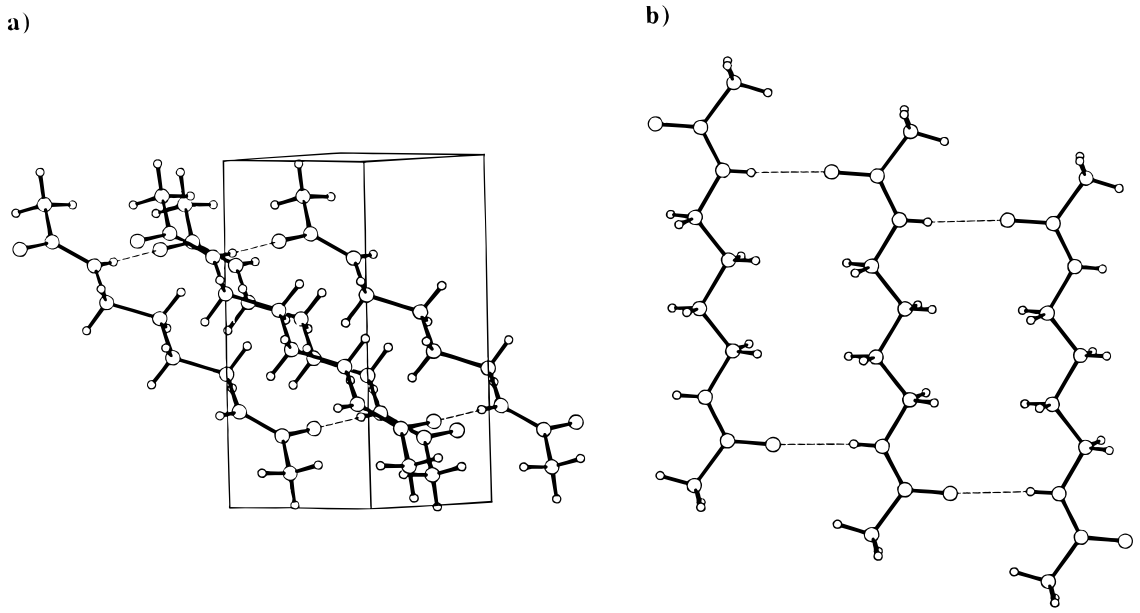

Figure 7. (a) Crystal packing of **aBUa**. The unit cell is shown by thinner lines, while the hydrogen bonds are indicated by dashed lines. The hydrogen bond system runs practically parallel to the *a* axis. (b) Perpendicular view to the amide planes of three hydrogen-bonded molecules. Note that the molecules are shifted in the molecular axis direction in order to improve the hydrogen bond geometry. The structure becomes very similar to the diamine moiety in the α form of nylons.

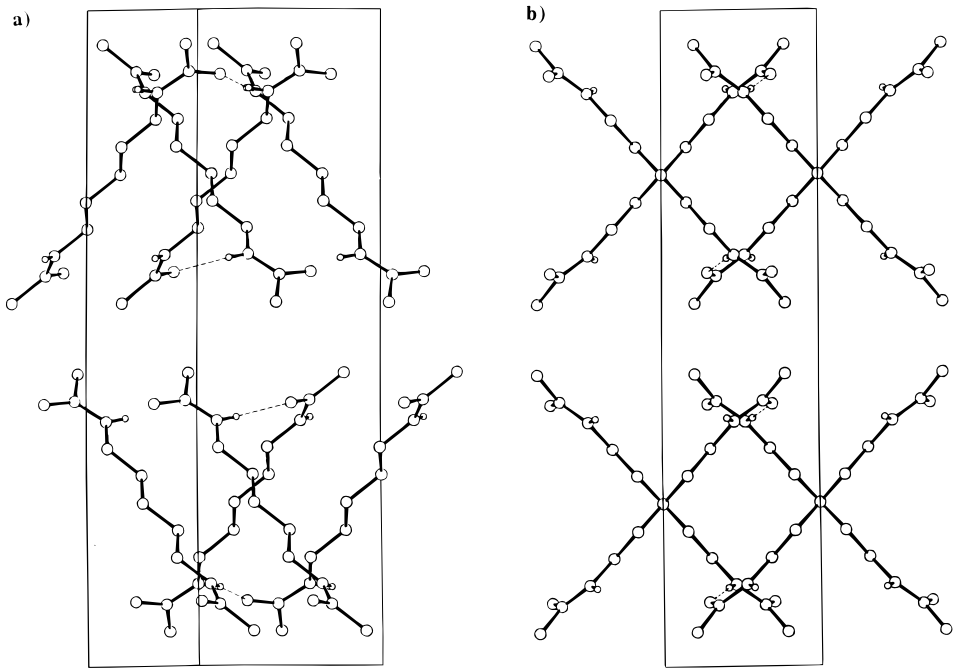

Figure 8. (a) Crystal packing of **aPEa**. The *c* axis is vertical in the figure. (b) Projection of the crystalline structure onto the *ac* plane. The mirror image molecules are at different levels in the *b* direction. Only the amide hydrogens are indicated in both figures.

lenediamide compounds also indicate that the φ_i torsion angles are rather variable. Thus, values close to the *trans* (173.41° and 169.46° for the *p,p′*-dimethoxy-*N,N′*-tetramethylenedibenzamide[39] and benzoic[40] derivatives), *skew* (119.98° for *p,p′*-dicyano-*N,N′*-tetramethylenedibenzamide[39]), and *gauche* (79.76° for *p,p′*-di-*tert*-butyl-*N,N′*-tetramethylenedibenzamide[39]) conformations have been experimentally observed.

Calculations on the **aBUa** molecule show that the conformation found for the **aETa** compound, which is related to the γ form of nylons, was characterized as a minimum ($\varphi_1 = -\varphi_1' = 86.8°$, $\nu_1 = -\nu_1 = 178.2°$, and $\nu_2 = 180.1°$), but not the *all-trans* conformation. However, the energy difference at the HF/6-31G(d) level between two such conformations was only 0.7 kcal/mol, whereas for **aPRa** it was 3 kcal/mol at the same computational level.

***N*-[5-(Acetylamino)pentamethylene]acetamide (aPEa).** aPEa crystallizes in a *Pbcb* space group, and the unit cell contains four molecules, two of which are identical and have the parameters given in Table 3. The other two molecules are related by glide planes and are their mirror images. Molecular symmetry is characterized by a binary axis through the central carbon atom and so both molecule halves have the same conformational angles. Hydrogen bonds with lengths and angles

within the standard range are formed between molecules related by a glide plane (Figure 8). It is worth noting that they are established along two directions ([110] and [$\bar{1}$10]) in a way similar to that of the new structures proposed for nylons with two hydrogen bond directions.[23,24] A ca. 30° rotation between the *CO* directions is also a conformational characteristic, and it is due to the slight deviation from the *all-trans* conformation of the φ_i torsion angles (−166.5°). A similar conformation has been reported for the dicarbonylic unit of nylon 6,5 in order to explain the two-directional hydrogen bond geometry.[23] In both cases an unfavorable geometry is expected for the *all-trans* conformation characteristic of the α form due to the odd number of methylenes in the diamine or diacid moieties. The influence of the groups attached to the carbonyl carbons is in this case manifest, since a *TGTG* conformation has been reported for the polymethylene segment in the dibenzamide derivative.[35] A projection of the structure is shown in Figure 8b. Note that there are two layers of molecules along the *c* crystal axis and that each layer is composed of both mirror images.

Conclusions

The results presented in this paper give the conformational data of the methylene segments in Ψ[NHCO] aliphatic diamides. These data complement the previous work on the conformational preferences of the methylene units when they are placed in the dicarbonylic moiety of the related diamides. Some relevant conclusions on the understanding of the conformational behavior can be inferred.

The *gauche* conformation characteristic of the dicarbonylic units has not been found as a general trend in the diamine moieties. On the contrary, a great conformational variability has been observed in the solid state for the different compounds studied. Moreover, theoretical calculations on isolated molecules show a great number of minimum-energy conformations for a given compound. The energy differences between them are low and strongly depend on the computational level due to the influence of electron correlation effects.

The crystal structure of the even diamides is characterized by a single hydrogen bond direction. The conformation is *all-trans* for the butylenediamine derivative and gives a structure similar to that of the α form of nylons. In the ethylenediamine derivative a particular conformation ($\varphi_1 = -\varphi_2 \sim 90°$) is characteristic and approaches to the γ form of nylons where *skew* bonds are present.

Odd diamides are interesting due to the unfavorable hydrogen bond geometry expected for a *trans* conformation. In fact, the propylenediamine derivative presents an asymmetric folded conformation in order to improve the hydrogen bonds. When the number of methylenes increases, the conformation approaches the extended one. Hence, a slight deviation from 180° (in the same direction) produces a good hydrogen bond system for the pentamethylenediamine derivative. Amide groups become rotated, and two hydrogen bond directions result in the crystal. Similar conformations have recently been postulated for nylons derived from diamines and diacids with an odd number of methylenes,[13,23,24] since the extended-chain conformation is expected to be energetically unfavored.

The computational analysis on isolated molecules predicts the solid-state conformation for the *N*-[2-(acetylamino)ethylene]acetamide compound. For all the compounds analyzed, the extended-chain conformation was not detected as a minimum energy in the respective potential energy hypersurface. However, their energy approaches the minimum when the number of methylene groups increases. So, differences of relative energies of 3.7 and 0.7 kcal/mol with respect to the minima predicted for the derivatives with two and four methylene groups were respectively computed at the HF/6-31G(d) level. These results are also in clear agreement with the solid-state observations.

Acknowledgment. The authors express their gratitude to Dr. V. Tereshko and Dr. X. Solans and to E. Escudero for her help with X-ray data collection and structure determination. The research was supported by DGICYT Grant PB93-1067. Authors are indebted to Centre de Supercomputació de Catalunya (CESCA) and Centre Europeu de Paralelisme de Barcelona (CEPBA) for computational facilities. E.N. acknowledges financial support from the Departament d'Ensenyament de la Generalitat de Catalunya.

Supporting Information Available: Crystallographic details, including Tables 7−12 of equivalent isotropic thermal parameters, bond lengths, and bond angles (6 pages). Ordering information is given on any current masthead page.

References and Notes

(1) Fernández-Santín, J. M.; Aymamí, J.; Rodríguez-Galán, A.; Muñoz-Guerra, S.; Subirana, J. A. *Nature (London)* **1984**, *311*, 53.
(2) Bella, J.; Alemán, C.; Fernández-Santín, J. M.; Alegre, C.; Subirana, J. A. *Macromolecules* **1992**, *25*, 5225.
(3) Puiggalí, J.; Muñoz-Guerra, S.; Lotz B. *Macromolecules* **1986**, *19*, 1119.
(4) Bella, J.; Puiggalí, J.; Subirana, J. A. *Polymer* **1994**, *35*, 1231.
(5) Puiggalí, J.; Subirana, J. A. *Polymeric Materials Encyclopedia*; Salomone, J. C., Ed.; CRC Press: Boca Raton, FL, 1996; Vol. 7, pp 5422−5432.
(6) Tormo, J.; Puiggalí, J.; Vives, J.; Fita, I.; Lloveras, J.; Bella, J.; Aymamí, J.; Subirana, J. A. *Biopolymers* **1992**, *32*, 643.
(7) Tereshko, V.; Vidal, X.; Goodman, M.; Subirana, J. A. *Macromolecules* **1995**, *28*, 264.
(8) Navarro, E.; Tereshko, V.; Subirana, J. A.; Puiggalí, J. *Biopolymers* **1995**, *36*, 711.
(9) Navarro, E.; Alemán, C.; Puiggalí, J. *J. Am. Chem. Soc.* **1995**, *117*, 7307.
(10) Alemán, C.; Navarro, E.; Puiggalí, J. *J. Org. Chem.* **1995**, *60*, 6135.
(11) Tereshko, V.; Navarro, E.; Puiggalí, J.; Subirana, J. A. *Macromolecules* **1993**, *26*, 7024.
(12) Navarro, E.; Puiggalí, J.; Subirana, J. A. *Macromol. Chem. Phys.* **1995**, *196*, 2361.
(13) Puiggalí, J.; Aceituno, J. E.; Navarro, E.; Campos, L.; Subirana, J. A. *Macromolecules* **1996**, *29*, 8170.
(14) Alemán, C.; Vega, M. C.; Navarro, E.; Puiggalí, J. *J. Pept. Sci.* **1996**, *2*, 364.
(15) Alemán, C.; Navarro, E.; Puiggalí, J. *J. Phys. Chem.* **1996**, *100*, 16131.
(16) Vega, M. C.; Alemán, C.; Navarro, E.; Puiggalí, J., submitted work.
(17) Allen, F. H.; Kennard, O.; Taylor, R. *Acc. Chem. Res.* **1983**, *16*, 46.
(18) Berstein, F. C.; Koetzle, O.; Williams, G. J. B.; Mayer, G. F.; Brice, M. D.; Rodgers, J. R.; Kennard, O.; Shimanouchi, T.; Tasumi, M. *J. Mol. Biol.* **1977**, *112*, 535.
(19) Wendoloski, J. J.; Gardner, J. K.; Hirschinger, J.; Miura, H.; English, A. B. *Science* **1990**, *247*, 431.
(20) Kohan, M. I. *Nylon plastics;* John Wiley and Sons: New York, 1973; pp 271−305.
(21) Atkins, E. D. T.; Hill, M. J.; Veluraja, K. *Polymer* **1994**, *36*, 35.
(22) Schmidt, G. F.; Stuart, H. A. *Z. Naturforsch.* **1958**, *13A*, 222.
(23) Navarro, E.; Franco, L.; Subirana, J. A.; Puiggalí, J. *Macromolecules* **1995**, *28*, 8742.

(24) Navarro, E.; Alemán, C.; Subirana, J. A.; Puiggalí, J. *Macromolecules* **1996**, *29*, 5406.
(25) Howard, J. C.; Ali, A.; Scheraga, H. A.; Momany, F. A. *Macromolecules* **1975**, *8*, 607.
(26) Sheldrick, G. M. *SHELXS-86. Program for Crystal Structure Determination* University of Oxford: Oxford, England, 1986.
(27) Sheldrick, G. M. *SHELXL-93. Program for Refinement of Crystal Structure;* Institut für Anorganische Chemie der Universitat Gottingen: Gottingen, Germany, 1993.
(28) Hatiharan, P. C.; Pople, J. A. *Theor. Chim. Acta* **1973**, *28*, 213.
(29) Møller, C.; Plesset, M. S. *Phys. Rev.* **1934**, *46*, 618.
(30) Frisch, M. J.; Trucks, G. W.; Schlegel, H. B.; Gill, P. M. W.; Johnson, B. G.; Robb, M. A.; Cheeseman, J. R.; Keith, T.; Petersson, G. A.; Montgomery, J. A.; Raghavachari, K.; Al-Laham, M. A.; Zakrzewski, V. G.; Ortiz, J. V.; Foresman, J. B.; Cioslowski, J.; Stefanov, B. B.; Nanayakkara, A.; Challacombe, M.; Peng, C. Y.; Ayala, P. Y.; Chen, W.; Wong, M. W.; Andrés, J. L.; Reploge, E. S.; Gomperts, R.; Martin, R. L.; Fox, D. J.; Binkley, J. S.; Defrees, D. J.; Baker, J.; Steward, J. P.; Head-Gordon, M.; González, C.; Pople, J. A. Gaussian-94, Revision D.2, Gaussian Inc., Pittsburgh PA, 1995.
(31) Palmer, A.; Brisse, F. *Acta Crystallogr., Sect. B* **1980**, *36*, 1447.
(32) Stephens, F. S.; Vagg, R. S. *Inorg.Chim. Acta* **1988**, *142*, 43.
(33) Glowka, M. L. *Acta Crystallogr., Sect. C* **1991**, *47*, 1680.
(34) (a) Sponer, J.; Leszczynski, J.; Hobza, P. *J. Comput. Chem.* **1996**, *17*, 841. (b) Hobza, P.; Sponer, J.; Polasek, M. *J. Am.Chem. Soc.* **1995**, *117*, 792.
(35) Brisson, J.; Brisse, F. *Macromolecules* **1986**, *19*, 2632.
(36) Benedetti, E.; Ciajolo, M. R.; Corradini, P. *Eur. Polym. J.* **1974**, *10*, 1201.
(37) Ciajolo, M. R.; Pavone, V.; Benedetti, E. *Acta Crystallogr., Sect. B* **1977**, *33*, 1295.
(38) Alemán, C.; Casanovas, J. *Biopolymers* **1995**, *36*, 71.
(39) Brisson, J.; Gagne, J.; Brisse, F. *Can J. Chem.* **1989**, *67*, 840.
(40) Harkema, S.; van Hummel, G. J.; Gaymans, R. J. *Acta Crystallogr., Sect. B* **1980**, *36*, 3182.

MA970243K